Wing Tilt Scheduling in Tandem-Wing VTOL Configurations

Kacper Grzędziński	**Valentin Stéphan**	**Argyrios Zolotas**
Research Fellow	Graduate Student	Reader in Systems and Control
Cranfield University	Cranfield University	Cranfield University
United Kingdom	United Kingdom	United Kingdom

ABSTRACT

The effect of scheduling wing tilt angle in tandem tilt-wing vertical take-off and landing (VTOL) aircraft is investigated with respect to both the static and dynamic longitudinal stability; a first-principles three degree of freedom model of longitudinal motion is derived and simulated with aerodynamic coefficients from a conventional subsonic aerofoil profile. Model trimming through readily available optimisation software is used to determine the values of thrusts and tilts needed for trimmed flight; at airspeeds that correspond to hover and cruise flight modes. The resulting equilibria are discussed qualitatively and compared to equilibria resulting from a model that accounts for the interaction between propeller slipstream and wing aerofoils. Through simulations, it is shown that propeller slipstream influences the dynamic longitudinal modes of the aircraft, under the parametric assumptions of this paper.

NOMENCLATURE

Symbol	Description	Unit
α	aerofoil angle of attack	rad
α_F	fuselage angle of attack	rad
$\tilde{\alpha}_j$	effective angle of attack, wing j	rad
γ	flight path angle	rad
δ_j	tilt angle, wing j	rad
θ	fuselage pitch angle	rad
c	wing chord	m
D_j	drag, wing j	N
$F_{x,j}^b$	horizontal force, body frame	N
$F_{z,j}^b$	vertical force, body frame	N
g	acceleration due to gravity	m/s^2
J	moment of inertia	kg m^2
$l_{x,f}$	horizontal arm, front wing	m
$l_{x,r}$	horizontal arm, rear wing	m
L_j	lift, wing j	N
M_a	Mach number	
$M_{ac,j}$	zero lift moment, wing j	N m
S_j	wing surface area	m^2
T_j	thrust, wing j	N
$\tilde{V}$	effective velocity magnitude	m/s
V_∞	freestream velocity magnitude	m/s
$\tilde{V}_x$	horizontal component of $\tilde{V}$	m/s
$\tilde{V}_z$	vertical component of $\tilde{V}$	m/s
$\dot{x}^i$	horizontal velocity, inertial	m/s
$\dot{z}^i$	vertical velocity, inertial	m/s

INTRODUCTION

Tilt-wing VTOL aircraft have the ability rotate their hinged wings to achieve powered lift without reliance on conventional aerodynamic surfaces. The merits and drawbacks of tilt-wings have been extensively studied in the past through experimental flight test programs, for many exotic airframe configurations (Ref. 1). However, controlling these complex aircraft, particularly during transition between forward flight and hover, is still a challenging technical problem owing to the nonlinearity and controllability of the flight dynamics (Ref. 2).

As in conventional aircraft, pitch authority is provided by mechanisms that are mounted on airframe extremities; a tail plane or canard in most cases, but also flow altering devices such as jet exhausts and propellers (Ref. 3). Tandem tilt-wings provide the additional degree of freedom to vary the tail plane tilt angle simultaneously. The choice of tilt schedules for the wing and tail plane are typically consolidated by tuning during flight envelope exploration and has received little attention in literature (Ref. 4).

In this work, we study the influence of wing tilting, as a control degree of freedom, for enabling trimmed flight conditions. The work is carried out based on an analytical approach for a conceptual UAM sized vehicle, across a range of horizontal airspeeds corresponding to hover and cruise flight configurations. This modelling framework captures the main coupling between the propulsors and airframe, as a precursor to design of sophisticated model-based multivariable control systems.

Attention is restricted to the longitudinal dynamics whilst accounting for propeller-wing slipstream interaction, unlike

PREPRINT

(Ref. 5). Most UAM sized tiltwing VTOL concepts have significant portions of the aerodynamic surfaces wetted by the propulsor slipstream. Prior literature has assumed the same wing and tail tilt angles in tandem configurations, particularly in more symmetrical geometries (Ref. 6). However, even small dissimilarity in wing tilt angles have significant effect on the aircraft's longitudinal stability, as is explicitly documented in (Ref. 5). We show how this is magnified by the presence of propulsor slipstream effects.

TILT-WING MODELLING

Free-body Diagram

This work is restricted to longitudinal dynamics, that is, three degrees of freedom including two orthogonal directions for translation and one for rotation. Positive sign conventions are depicted in Fig. 1, for an aircraft with two tiltable wings that are forward (front) and aft (rear) of the centre of gravity (CG).
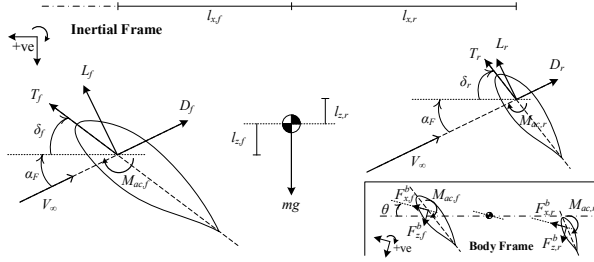
Figure 1. Free body diagram of longitudinal motion without propeller induced flow.

To synthesise a control-oriented model for control system design, we employ the following set of assumptions.

Assumptions

1. Rigid-body motion in the longitudinal plane.
2. Tilt axes coincide with aerofoil aerodynamic centres (ACs).
3. Axially induced propulsor slipstream flow only, which affects the entire wing surface area.
4. Constant mass m and negligible change of CG position as the wings tilt.
5. Gyroscopic moments ignored.
6. Propulsor thrusts act from respective ACs.
7. Fuselage aerodynamics are ignored.
8. International standard atmosphere conditions.

Dynamic Equations

The differential equations for translating motion, derived from considering forces in the flat-earth inertial reference frame are as follows:

Author contact: Kacper Grzędziński, k.grzedzinski@cranfield.ac.uk

$$m \begin{bmatrix} \ddot{x}^i \\ \ddot{z}^i \end{bmatrix} = \begin{bmatrix} 0 \\ mg \end{bmatrix} + R_{ib}(\theta)\left(\begin{bmatrix} F_{x,f}^b \\ F_{z,f}^b \end{bmatrix} + \begin{bmatrix} F_{x,r}^b \\ F_{z,r}^b \end{bmatrix} \right), \quad (1)$$

$$\begin{bmatrix} F_{x,j}^b \\ F_{z,j}^b \end{bmatrix} = R_{bt}(\delta_j)\begin{bmatrix} T_j \\ 0 \end{bmatrix} + R_{bw}(\alpha_F)\begin{bmatrix} D_j(.) \\ L_j(.) \end{bmatrix}, \quad (2)$$

where the subscript j is used to distinguish between forces and angles that are caused by either the front (f) or rear (r) wing. The differential equation for rotational dynamics about the aircraft's centre of gravity are

$$J\ddot{\theta} = \begin{bmatrix} F_{x,f}^b & F_{z,f}^b \end{bmatrix} \cdot \begin{bmatrix} l_{z,f} \\ -l_{x,f} \end{bmatrix} + M_{ac,f} \quad (3)$$

$$+ \begin{bmatrix} F_{x,r}^b & F_{z,r}^b \end{bmatrix} \cdot \begin{bmatrix} -l_{z,r} \\ l_{x,r} \end{bmatrix} + M_{ac,r},$$

with aerodynamic forces, moments and dynamic pressure:

$$L = QSC_L(\alpha, M_a), \quad (4)$$

$$D = QSC_D(\alpha, M_a), \quad (5)$$

$$M = QSc\,C_M(\alpha, M_a), \quad (6)$$

$$Q = \frac{1}{2}\rho V^2. \quad (7)$$

All forces are transformed through appropriate rotation matrices into the inertial reference frame; firstly, originating in the wind frame (aerodynamic forces) or tilted wing frame (propulsive forces); then transformed into the body frame, and finally into the inertial reference frame:

$$R_{bw}(\alpha) = \begin{bmatrix} -\cos\alpha & \sin\alpha \\ -\sin\alpha & -\cos\alpha \end{bmatrix}, \quad (8)$$

$$R_{ib}(\theta) = \begin{bmatrix} \cos\theta & \sin\theta \\ -\sin\theta & \cos\theta \end{bmatrix}, \quad (9)$$

$$R_{bt}(\delta) = \begin{bmatrix} \cos\delta & \sin\delta \\ -\sin\delta & \cos\delta \end{bmatrix}. \quad (10)$$

The fuselage angle of attack

$$\alpha_F = \theta - \gamma \quad (11)$$

is used to translate forces from the wind frame to the body frame, with the flight path angle definition

$$\gamma = -\arctan\frac{\dot{z}^i}{\dot{x}^i}. \quad (12)$$

Induced Propeller Flow

The approximation of induced flow by the propulsors is the key feature of this model. In reality, the aerodynamics are highly complicated and dependent on localised geometry and many other factors that are out of scope of this paper; we use a simple approach that is also utilised to study two-dimensional flow in turbomachinery (Ref. 7).

Based on momentum theory (Ref. 8), the induced flow imparted by a propeller disk onto the stream directly behind the propeller can be described by

$$V_i = \left(-\frac{V_{\perp\infty}}{2} + \sqrt{\frac{V_{\perp\infty}^2}{4} + \frac{T}{2\rho A_{disk}}} \right), \qquad (13)$$

where the freestream component that enters the propeller disk A_{disk}, in the case of the tiltable wings, is

$$V_{\perp\infty} = V_\infty \cos(\alpha_F + \delta). \qquad (14)$$

The propeller induced flow affects the aerodynamic forces in two ways: firstly, by local increase of dynamic pressure; secondly, a local change in angle of attack. Hence, the propulsor slipstream effects will change the static and dynamic behaviour.
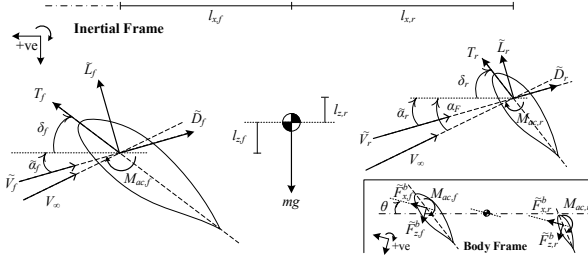
Figure 2. Free body diagram considering the aircraft's longitudinal motion with propeller induced flow.

With the reference frames defined as in Figure 2, the effective freestream velocity $\tilde{V}$ experienced by each aerofoil respectively can be derived from appropriately considering the respective velocity diagrams. Both aerofoils will share the same freestream velocity V_∞, but will have induced velocities depending on (13). The resulting effective dynamic pressure experienced by an aerofoil in a slipstream is therefore

$$\tilde{Q} = \frac{1}{2}\rho\tilde{V}^2. \qquad (15)$$

The effective angle of attack between the fuselage and the effective wind $\tilde{V}$ are computed using the modified equations:

$$\tilde{\alpha} = \theta - \tilde{\gamma}, \qquad (16)$$

$$\tilde{\gamma} = \arctan\frac{\tilde{V}_z}{\tilde{V}_x}, \quad \tilde{V} = \sqrt{\tilde{V}_x^2 + \tilde{V}_z^2}, \qquad (17),(18)$$

$$\tilde{V}_x = V_\infty \cos\gamma + V_i \cos(\theta + \delta), \qquad (19)$$

$$\tilde{V}_z = V_\infty \sin\gamma + V_i \sin(\theta + \delta). \qquad (20)$$

The effective *aerofoil* angle of attack must also take into account the additional tilt relative to the fuselage

$$\alpha = \tilde{\alpha} + \delta. \qquad (21)$$

Airframe Parameters

Table 1. Conceptual tilt-wing aircraft simulation parameters.

Characteristic	Value (Unit)
Front Wing Area	16.0 m^2
Rear Wing Area	2.29 m^2
Wing Chords	1.5 m
AC to AC Length ($l_{x,f}+l_{x,r}$)	6.0 m
Front, Rear Propeller Ø	2.0, 1.2 m
Vertical Arms $l_{z,f}$, $l_{z,r}$	0, 0 m
Thrust Limits	0≤ T_j≤30,000 N
Tilt Limits	-5 ≤ δ_j ≤ 95 deg
Total Mass	2,205 kg
Inertia	1,824 kg m^2
CG Location ($l_{x,r}$)	5.4 m
Altitude	1 km
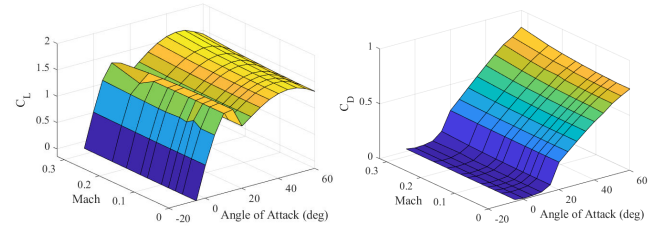
Figure 3. Lift and drag coefficients for both front and rear wing aerofoils.

Based on the expressions of this section, the dynamics of the aircraft are implicitly described by the state-space system

$$\dot{x} = f(x, u), \qquad (22)$$

where $x = \left[\dot{x}^i, \dot{z}^i, \theta, \dot{\theta}\right]^T$ is the state vector and $u = \left[T_r, T_f, \delta_r, \delta_f\right]^T$ is the input vector of available control degrees of freedom.

The main limitation of this model is that it does not consider damping terms. Whilst these parameters do affect dynamic stability (Ref. 9), we focus on showing the effect of propeller slipstream on stability, independently of pitch damping. Moreover, the induced velocity term (13) is conservative as it does not account for the contraction of the slipstream tube during low propeller loading; the induced velocity can double in magnitude during flight conditions where the aircraft is at high airspeed and relatively low thrust (Ref. 8).

TRIMMING

Conditions for Trimming

Trimmed aircraft conditions are obtained when the equilibria pairs of states x_e and inputs u_e satisfy

$$f(x_e, u_e) = [0, 0, 0, 0]^T. \qquad (23)$$

To explore a range of operating conditions that exercise the available tilting degrees of freedom, the models are trimmed at horizontal airspeeds $\dot{x}_e^i$ from 1 to 120 m/s. Vertical airspeed, pitch and pitch rate are all constrained to be zero. Such conditions capture transitions between hover and cruise flight where no altitude is lost and where the aircraft longitudinal axis remains parallel to the ground.

Obtaining flight conditions for a range of x_e requires a trimming exercise to find the corresponding u_e:

$$u_e = \arg \min_{[T_r, T_f, \delta_r, \delta_f]^T} T_r + T_f \qquad (24)$$

subject to:
$$f(x, u) = [0, 0, 0, 0]^T$$
$$x = [\dot{x}_e^i, 0, 0, 0]^T$$
$$\underline{T} \leqslant T_j \leqslant \overline{T}$$
$$\underline{\delta} \leqslant \delta_j \leqslant \overline{\delta}$$

Since this is a nonlinear optimisation, there is no guarantee that the optimiser will be unique; it depends on the solver's initialisation and several parameters outside the scope of this paper. However, the optimisation can be initialised and validated at known conditions based on simple static analysis. For example, for the no induced flow scenario at zero m/s (hover), the inputs can be easily computed through a simple moment balance around the CG. This method is used to initialise the trimming optimisation. The remaining trim point optimisations are initialised with the inputs of the previously solved optimisation, starting from hover.

It is important to highlight that this optimisation's cost function only penalises the use of thrust; tilt angles are free to be set to any value with no contribution to the cost function. Hence, the trimming exercise finds steady-state level conditions which minimise total thrust usage.

This scenario could physically represent a strict approach/exit corridor for a vertiport in an urban environment, where altitude is kept constant before vertical landing or transitioning to horizontal flight. In practice, pitch angle does not have to be strictly forced to zero, but it is chosen to enable fairer comparison between the baseline model and the propeller slipstream modelling.

The trimming exercise is conducted on two tilt-wing aircraft models:

1. The tilt-wing model without propulsor slipstream effects (Fig. 1);

$$\dot{x} = \bar{f}(x, u) \qquad (25)$$

i.e. the implicit state-space representation of equations (1), and (3) with forces (2), (4) and (5) that utilise arguments

$$Q_\infty = \frac{1}{2} \rho V_\infty^2, \qquad \alpha_j = \alpha_F + \delta_j. \qquad (26), (27)$$

2. The tilt-wing model with propulsor slipstream effects (Fig. 2);

$$\dot{x} = \tilde{f}(x, u) \qquad (28)$$

i.e. the implicit state-space representation of equation (1) with modified (2) which yields

$$m \begin{bmatrix} \ddot{x}^i \\ \ddot{z}^i \end{bmatrix} = \begin{bmatrix} 0 \\ mg \end{bmatrix} + R_{ib}(\theta) \left(\begin{bmatrix} \tilde{F}_{x,f}^b \\ \tilde{F}_{z,f}^b \end{bmatrix} + \begin{bmatrix} \tilde{F}_{x,r}^b \\ \tilde{F}_{z,r}^b \end{bmatrix} \right), \qquad (29)$$

$$\begin{bmatrix} \tilde{F}_{x,j}^b \\ \tilde{F}_{z,j}^b \end{bmatrix} = R_{bt}(\delta_j) \begin{bmatrix} T_j \\ 0 \end{bmatrix} + R_{bw}(\tilde{\alpha}_j) \begin{bmatrix} \tilde{D}_j(.) \\ \tilde{L}_j(.) \end{bmatrix}, \qquad (30)$$

and (3), with specialised aerodynamic forces (4) and (5) that utilise arguments

$$\tilde{Q}_j = \frac{1}{2} \rho \tilde{V}_j^2, \qquad \alpha_j = \tilde{\alpha}_j + \delta_j. \qquad (31), (32)$$

Note that α_F is still used in this modelling scenario since $\tilde{V}_j$ requires computation of (14).

Static Longitudinal Stability

Static longitudinal stability is checked by inspecting whether the condition

$$\frac{dC_M}{d\alpha_F} < 0 \qquad (33)$$

holds for a range of perturbations in α_F. These perturbations are made by varying pitch angle for each of the considered trimmed conditions (see Fig. 4).

Linearisation

Dynamic stability is analysed by inspecting the linearisation of (25) and (28) at each trimmed flight condition. The local state and input behaviour around each equilibrium is described by

$$\Delta \dot{x} = A \Delta x + B \Delta u \qquad (34)$$

such that the behaviour of the system near each equilibrium point is approximately

$$x \approx x_e + \Delta x, \qquad u \approx u_e + \Delta u. \qquad (35), (36)$$

The open-loop dynamic modes: the short-mode and phugoid, can be analysed by inspecting the eigenvalues of matrix A. Dynamic longitudinal stability at an equilibrium is implied if all eigenvalues of matrix A are strictly negative.
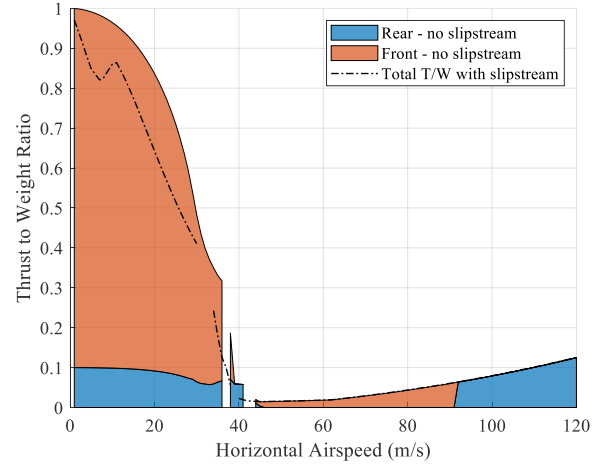
RESULTS

The following plots compare the results of trimming model 1 against model 2; with slipstream effects due to four propellers on the front wing and two propellers on the rear wing.
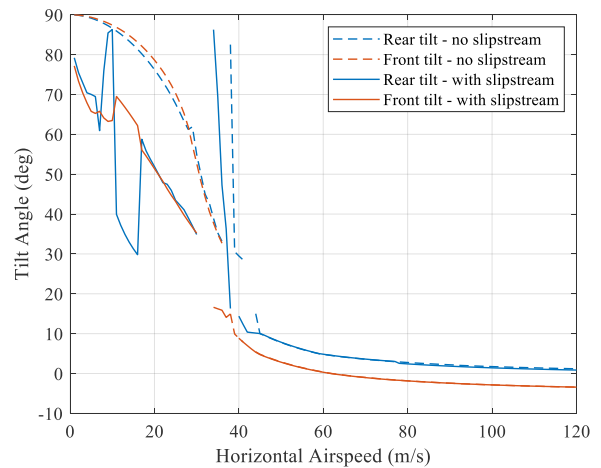
Static Longitudinal Stability
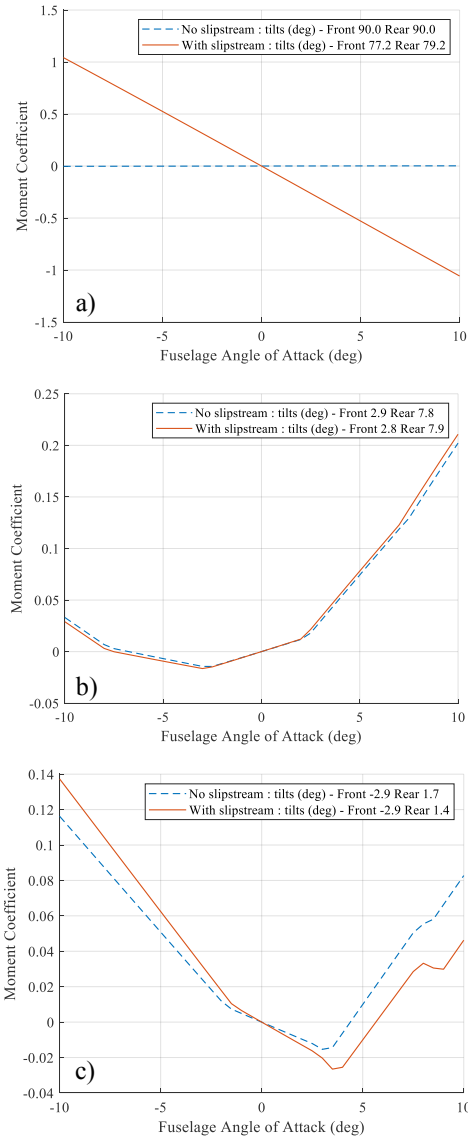
Figure 4. Moment coefficients against fuselage angle of attack; trim conditions a) 1 m/s, b) 50 m/s, c) 100 m/s.

Figure 5. Thrust to weight ratio for trimmed flight using model 1; no slipstream effects.
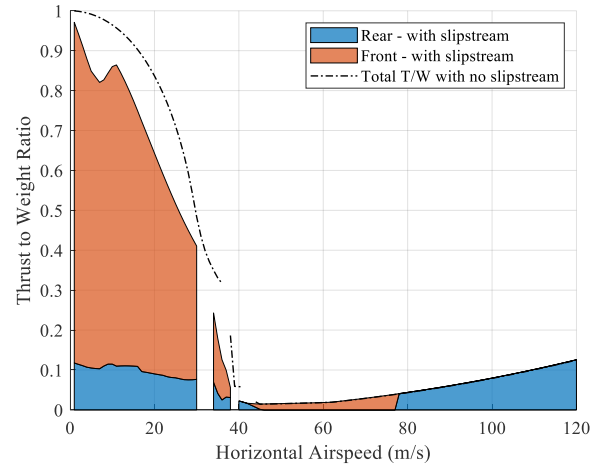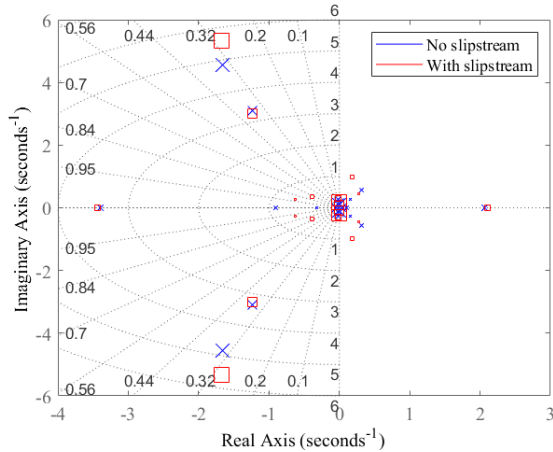

**Figure 6. Thrust to weight ratio for trimmed flight using model 2; with slipstream effects.**

Figure 7. Tilt angle schedule for trimmed flight.

5

Dynamic Longitudinal Stability

Figure 8. Pole map of five trimmed conditions: 100, 75, 50, 25 and 1 m/s. Logarithmically scaled symbols denote poles at each condition, in descending order. Lines of constant damping ratio radiate from origin.
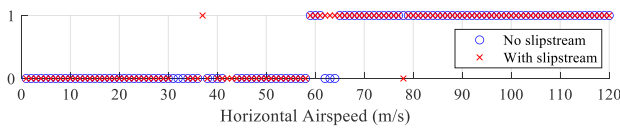
Figure 9. Stability of linearised dynamics over range horizontal airspeeds; boolean ones denote stability.

General Observations

- Less thrust is required during hover and slow flight due to additional blown lift from the slipstreams.
- Speeds between 30 and 40 m/s are problematic for numerical trimming; this coincides with transition from high to low drag conditions and may arise from the chosen aircraft parameters and solver.
- Tilt angles are practically the same for high speed flight for both modelling cases. This is an expected result since propeller induced slipstream velocities are small compared to the airspeed at fast cruise conditions.
- Low speed cruise favours use of front wing thrust whereas high speed cruise favours rear wing thrust for total minimum thrust use.
- Despite the same thrust required for both models during high speed cruise, the preference of rear wing thrust occurs at different values; approximately 90 m/s and 78 m/s without slipstream and with slipstream effects respectively.
- Pole locations at low airspeeds are significantly different between the two modelling approaches.
- In general, all dynamic modes are stable above horizontal airspeeds of 59 m/s, regardless of modelling method. Some outliers are present most likely due to numerical tolerances.

No Slipstream Modelling

- Tilt angles for trimmed conditions are approximately equal during low-speed hover/transition, unlike for high speed flight conditions.

With Slipstream Modelling

- Between 18 and 30 m/s, tilt angles for trim are approximately equal unlike lower speeds (4 to 18 m/s) where the tilt angles vary unintuitively.

CONCLUSIONS

Longitudinal stability of a tilt-wing aircraft model has been analysed, where propulsor and wing slipstream interaction is accounted for using analytical methods. We show the non-intuitive nature of tilt angle scheduling for trimmed level flight, highlighting the need to account for such phenomena.

REFERENCES

1. Saeed, A. S., Younes, A. B., Islam, S., Dias, J., Seneviratne, L., and Cai, G., "A review on the platform design, dynamic modeling and control of hybrid UAVs," 2015 International Conference on Unmanned Aircraft Systems (ICUAS), 2015, pp. 806–815.

2. Naldi, R., and Marconi, L., "Optimal transition maneuvers for a class of V/STOL aircraft," *Automatica*, Vol. 47, (5), 2011, pp. 870–879.

3. Rubin, F., "Modelling & Analysis of a Tilt Wing Aircraft," KTH Sweden, 2018, URL: http://kth.diva-portal.org/smash/record.jsf?pid=diva2%3A1292412&dswid=4161

4. Fredericks, W. J., Mcswain, R. G., Beaton, B. F., Klassman, D. W., and Theodore, C. R., "Greased Lightning (GL-10) Flight Testing Campaign," NASA Report 20170007194, 2017, URL: https://ntrs.nasa.gov/citations/20170007194

5. Beyer, Y., Krüger, T., Krüger, A., Steen, M., Hecker, P., "Simulation and Control of a Tandem Tiltwing RPAS Without Experimental Data," 9th International Micro Air Vehicles Conference, 2017.

6. Chauhan, S. S., and Martins, J. R. R. A., "Tilt-wing eVTOL takeoff trajectory optimization," *Journal of Aircaft*, Vol. 57, (1), 2020, pp. 93–112.

7. Saravanamuttoo, H. I. H., Rogers, G. F. C., Cohen, H., and Straznicky, P. V., *Gas Turbine Theory*, 6th ed., 2009.

8. Selig, M., "Modeling Full-Envelope Aerodynamics of Small UAVs in Realtime," AIAA Atmospheric Flight Mechanics Conference, 2010.

9. Weinacht, P., "Navier-Stokes Predictions of the Individual Components of the Pitch-Damping Sum," *Journal of Spacecraft and Rockets*, Vol. 35, (5), Sep. 1998, pp. 598–605.

2021-01

Wing tilt scheduling in tandem-wing VTOL configurations

þÿ G r z   d z i D s k i ,   K a c p e r

Vertical Flight Society (American Helicopter Society)